

See discussions, stats, and author profiles for this publication at: <https://www.researchgate.net/publication/230705341>

# Inward Cationic Diffusion and Formation of Silica-Rich Surface Nanolayer of Glass

ARTICLE in CHEMISTRY OF MATERIALS · APRIL 2009

Impact Factor: 8.35 · DOI: 10.1021/cm802513r

---

CITATIONS

26

---

READS

34

## 3 AUTHORS:



**Morten M Smedskjaer**

Aalborg University

79 PUBLICATIONS 790 CITATIONS

SEE PROFILE



**Joachim Deubener**

Technische Universität Clausthal

109 PUBLICATIONS 1,170 CITATIONS

SEE PROFILE



**Yuanzheng Yue**

Aalborg University

209 PUBLICATIONS 2,715 CITATIONS

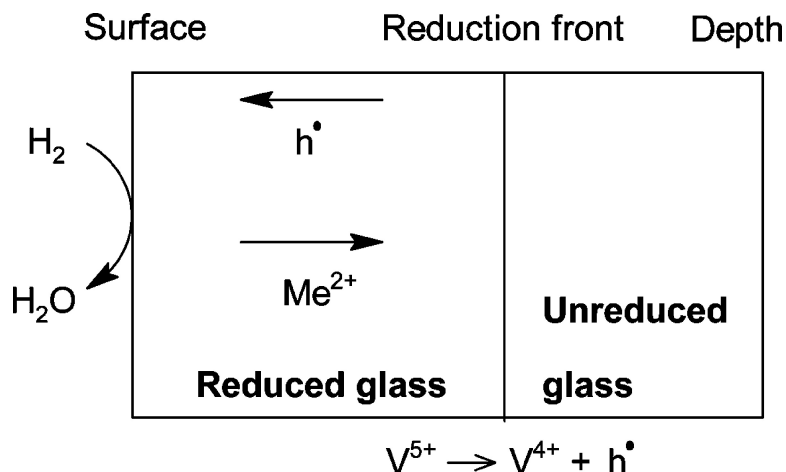
SEE PROFILE

## Inward Cationic Diffusion and Formation of Silica-Rich Surface Nanolayer of Glass

Morten M. Smedskjaer, Joachim Deubener, and Yuanzheng Yue

*Chem. Mater.*, **2009**, 21 (7), 1242-1247 • DOI: 10.1021/cm802513r • Publication Date (Web): 03 March 2009

Downloaded from <http://pubs.acs.org> on April 7, 2009



### More About This Article

Additional resources and features associated with this article are available within the HTML version:

- Supporting Information
- Access to high resolution figures
- Links to articles and content related to this article
- Copyright permission to reproduce figures and/or text from this article

[View the Full Text HTML](#)



**ACS Publications**  
High quality. High impact.

# Inward Cationic Diffusion and Formation of Silica-Rich Surface Nanolayer of Glass

Morten M. Smedskjaer,<sup>†</sup> Joachim Deubener,<sup>‡</sup> and Yuanzheng Yue<sup>\*,†</sup>

Section of Chemistry, Aalborg University, DK-9000 Aalborg, Denmark, and Institute of Non-Metallic Materials, Clausthal University of Technology, D-38678 Clausthal-Zellerfeld, Germany

Received September 17, 2008. Revised Manuscript Received December 4, 2008

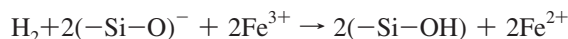
This paper reports a chemical approach for obtaining a silica-rich nanolayer on the surface of a vanadium-bearing silicate glass. The approach involves depletion of earth alkaline ions ( $\text{Mg}^{2+}$  and  $\text{Ca}^{2+}$ ) from the glass surface by means of inward diffusion of those ions, i.e., diffusion from the surface to the interior of the glass. The inward diffusion is induced by the reduction of  $\text{V}^{5+}$  to  $\text{V}^{4+}$  ions, when the glass is heat-treated in  $\text{H}_2/\text{N}_2$  (1/99 v/v) at the glass transition temperature ( $T_g$ ) for certain durations ( $t_a$ ). During the reduction of vanadium by  $\text{H}_2$ , structurally bonded hydroxyl groups form and are incorporated into the glass structure. Both the  $\text{V}^{4+}$  and the hydroxyl contents increase with increasing  $t_a$  and hydrogen partial pressure. The inward diffusion enhances the hardness of the glass surface. The mechanism of the inward diffusion is suggested on the basis of a model describing the outward diffusion. The new approach provides a possibility to create a silica-rich nanolayer on glass surfaces by means of the inward diffusion process.

## 1. Introduction

The surface composition and structure of a glass have a crucial impact on the glass properties. There are different ways to modify the surface composition and structure, e.g., coating of metal oxides or polymers, chemical or physical vapor deposition, ion exchange between glass and salt melt, fire polishing, and so on. In the present paper, we attempt to modify the surface of a silicate glass via a new chemical route, i.e., to reduce polyvalent ions by using hydrogen gas and thereby induce inward diffusion (from surface to interior) of earth alkaline ions, and consequently to form a silica-rich surface layer. The resulting glass should possess surface properties approaching those of pure  $\text{SiO}_2$  glass, e.g., high hardness, low coefficient of thermal expansion, and high chemical durability. However, the glass does not need to be prepared at the high temperature normally required for producing  $\text{SiO}_2$  glass. The glasses with the silica-rich surface layer could be applied as, for example, ampoules for drugs, which demand high chemical durability. In addition, the modified surface could enhance the chemical bonding of an externally coated film to the glass and, hence, improve performances of the film.

Reaction between  $\text{H}_2$  and various polyvalent cations in glasses has been reported in the literature, e.g., reaction of  $\text{H}_2$  with  $\text{Fe}^{3+}$ ,<sup>1–3</sup>  $\text{Ag}^+$ ,<sup>4</sup>  $\text{Ce}^{4+}$ ,  $\text{Sn}^{4+}$ ,<sup>1</sup>  $\text{Cu}^{2+}$  or  $\text{Cu}^+$ ,<sup>5</sup>  $\text{Ni}^{2+}$ ,<sup>6</sup>

and penta- or trivalent As, Bi, and Sb.<sup>7</sup> Those cations are reduced to a lower valence state, whereas protons in the form of hydroxyl are introduced into the glass structure. The reduction process can often be described by the tarnishing model.<sup>4,8–10</sup> The model assumes that the reaction between the diffusing  $\text{H}_2$  gas molecules and the polyvalent ions is fast compared with the permeation (dissolution and diffusion) rate of  $\text{H}_2$ . In the case of reduction of  $\text{Fe}^{3+}$  to  $\text{Fe}^{2+}$ , the reaction can be written as



However, we have recently shown that besides the above-mentioned  $\text{H}_2$  permeation process, a diffusion process of electron holes ( $h^\bullet$ ) is involved in the reduction of  $\text{Fe}^{3+}$  to  $\text{Fe}^{2+}$ .<sup>3</sup> The process is a mirror-image of the  $\text{Fe}^{2+}$  oxidation mechanism in atmospheric air (see Figure 1a) that has been described in numerous studies.<sup>11–18</sup> One might expect the

\* Corresponding author. Tel.: 45 99408522. Fax: 45 96350558. E-mail: yy@bio.aau.dk.

<sup>†</sup> Aalborg University.

<sup>‡</sup> Clausthal University of Technology.

(1) Johnston, W. D.; Chelko, A. J. *J. Am. Ceram. Soc.* **1970**, *53*, 295.

(2) Gaillard, F.; Schmidt, B.; Mackwell, S.; McCammon, C. *Geochim. Cosmochim. Acta* **2003**, *67*, 2427.

(3) Smedskjaer, M. M. Master's thesis, Aalborg University, Aalborg, Denmark, 2008.

(4) Barton, J. L.; Morain, M. *J. Non-Cryst. Solids* **1970**, *3*, 115.

(5) Estournès, C.; Cornu, N.; Guille, J. L. *J. Non-Cryst. Solids* **1994**, *170*, 287.

(6) Estournès, C.; Lutz, T.; Guille, J. L. *J. Non-Cryst. Solids* **1996**, *197*, 192.

(7) Tuzzolo, M. R.; Shelby, J. E. *J. Non-Cryst. Solids* **1992**, *143*, 181.

(8) Crank, J. *The Mathematics of Diffusion*; Clarendon: Oxford, U.K., 1975.

(9) Shelby, J. E. *J. Appl. Phys.* **1980**, *51*, 2589.

(10) Shelby, J. E.; Vitko, J. J. *Non-Cryst. Solids* **1981**, *45*, 83.

(11) Cook, G. B.; Cooper, R. F.; Wu, T. J. *Non-Cryst. Solids* **1990**, *120*, 207.

(12) Cooper, R. F.; Fanselow, J. B.; Poker, D. B. *Geochim. Cosmochim. Acta* **1996**, *60*, 3253.

(13) Yue, Y. Z.; Korsgaard, M.; Kirkegaard, L. F.; Heide, G. *J. Am. Ceram. Soc.* **2009**, *92*, 62.

(14) Cooper, R. F.; Fanselow, J. B.; Weber, J. K. R.; Merkley, D. R.; Poker, D. B. *Science* **1996**, *274*, 1173.

(15) Smith, D. R.; Cooper, R. F. *J. Non-Cryst. Solids* **2000**, *278*, 145.

(16) Cook, G. B.; Cooper, R. F. *Am. Mineral.* **2000**, *85*, 397.

(17) Burkhard, D. J. M. *J. Petrol.* **2001**, *42*, 507.

(18) Magnien, V.; Neuville, D. R.; Cormier, L.; Roux, J.; Hazemann, J.-L.; de Ligny, D.; Pascarelli, S.; Vickridge, I.; Pinet, O.; Richet, P. *Geochim. Cosmochim. Acta* **2008**, *72*, 2157.

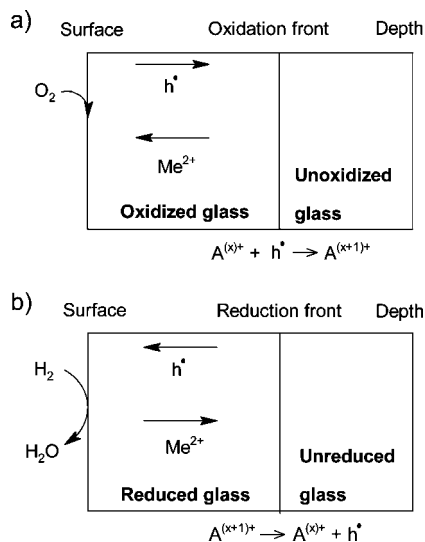


**Figure 1.** Schematic representation of mechanism of diffusion processes for two cases: (a) oxidation and (b) reduction of a polyvalent cation.  $\text{Me}^{2+}$  is a network-modifying cation,  $h^\bullet$  is an electron hole, and  $A$  is a polyvalent element.

diffusion of oxygen to dominate the redox kinetics. However, this only occurs above the liquidus temperature.<sup>18</sup> Instead, diffusion of electron holes and divalent cations (including  $\text{Fe}^{2+}$ ) dominates the redox kinetics. The motion of electron holes dissipates the driving force (Gibbs free energy of the redox reaction). But to maintain charge neutrality, the motion of electron holes is charge-coupled with the motion of network-modifying cations in the opposite direction. Divalent cation diffusion from the oxidation front to the surface becomes rate-limiting for the oxidation.<sup>12</sup>

In the case of reduction, the internal reduction of the polyvalent cation generates  $h^\bullet$ . These are filled by electrons released by ionic oxygen at the surface since oxygen is released into the reducing atmosphere as  $\text{H}_2\text{O}$ . The electron holes diffuse toward the surface, the flux of which is charge-balanced by an inward flux of the divalent cations (Figure 1b). This is a mirror-image of the oxidation mechanism (Figure 1a).<sup>12</sup> The outward diffusion of the electron holes occurs via the inward electron transfer from the low to the high valence state ions. Hence, the inward diffusion is driven by reduction of the high valence to the low valence state of the polyvalent cation. The network-modifying cations diffuse from the surface toward the interior, whereas the network-forming  $\text{Si}^{4+}$  ions do not diffuse because of their strong bonds to oxygen ions. This leads to formation of a silica-rich surface layer.<sup>3</sup>

To the best of our knowledge, the reduction of vanadium in glass by hydrogen and the resulting inward diffusion have not been investigated yet. Hence, it is interesting to find out whether the reduction of vanadium can be described by the tarnishing model, or by the inward diffusion model of cations, or a combined model. In this paper, we perform heat-treatments on a vanadium-bearing silicate glass at temperatures around the glass transition temperature ( $T_g$ ) for various durations ( $t_a$ ) in  $\text{H}_2/\text{N}_2$  gas mixtures with  $\text{H}_2$  partial pressures of 0.01 and 0.10 bar, respectively.  $T_g$  is the onset temperature at which a glass transforms into a liquid.<sup>19</sup> We determine the extent of the redox reactions by using ultraviolet–visible–

near-infrared (UV–vis–NIR) and Fourier transform infrared (FT-IR) spectroscopy, and the extent of diffusion by using secondary neutral mass spectroscopy (SNMS). Finally, to see how glass properties respond to the reduction of vanadium and to the resulting diffusion process, we measure the hardness and  $T_g$  of both thermally untreated and treated glasses.

## 2. Experimental Section

**2.1. Sample Preparation and Thermal Treatment.** The glass was prepared from  $\text{SiO}_2$  (purum p.a., Sigma-Aldrich),  $\text{CaCO}_3$  ( $\geq 99.5\%$ , Merck),  $\text{Mg}(\text{OH})_2 \cdot (\text{MgCO}_3)_4 \cdot (\text{H}_2\text{O})_5$  ( $\geq 99.99\%$  Aldrich),  $\text{Na}_2\text{CO}_3$  ( $\geq 99.9\%$ , Merck), and  $\text{V}_2\text{O}_5$  ( $\geq 99.0\%$ , Merck) powders. The batch was mixed and melted in air at  $1500^\circ\text{C}$  in an electrical furnace. The glass melt was then quenched on a brass plate and annealed in air at  $650^\circ\text{C}$  for 1 h. The composition of the glass was determined by X-ray fluorescence (XRF) to be (in wt %)  $\text{SiO}_2$  72.7%,  $\text{CaO}$  11.4%,  $\text{MgO}$  10.0%,  $\text{Na}_2\text{O}$  4.7%,  $\text{V}_2\text{O}_5$  1.0%. The main impurities were  $\text{Al}_2\text{O}_3$  0.3%,  $\text{K}_2\text{O}$  0.08%,  $\text{Fe}_2\text{O}_3$  0.07%,  $\text{TiO}_2$  0.02%. X-ray diffraction spectroscopy (XRD) carried out using a spectrometer at the  $\text{Cu K}\alpha$ -line did not show the presence of crystalline phases in the glass. The  $T_g$  of the glass was determined to be  $653^\circ\text{C}$  using differential scanning calorimetry (Netzsch STA 449C Jupiter).<sup>19</sup>

Cylindrical glass samples (diameter 8–10 mm; thickness 3 mm) were prepared from glass plates using a diamond drill. The samples for SNMS and hardness measurements were ground flat on one surface to a thickness of  $\sim 2$  mm by a six-step procedure with SiC paper under ethanol. Since diffusion depths below  $1\ \mu\text{m}$  are expected,<sup>3</sup> the surfaces were afterward carefully polished on a lapping machine using 3, 2, and  $1\ \mu\text{m}$  diamond paste and finally cleaned with acetone. The samples for UV–vis–NIR and FT-IR spectroscopy measurements were ground coplanar to achieve uniform thickness, and then they were polished to a thickness of 0.2 mm using the above-mentioned procedure. Care was required during the sample preparation procedure as small bubbles and/or lack of uniformity of thickness affect the absorbance measurements.

Some of the glass samples were heat-treated under a flow of  $\text{H}_2/\text{N}_2$  (1/99 v/v) gas at 1 atm using an electrical furnace. The samples were inserted into the cold furnace and the gas-flow was turned on. Heating and cooling of the samples were conducted at 10 K/min. The samples were held at the  $T_g$  for various heat-treatment durations. In addition, some of the samples were heat-treated in  $\text{H}_2/\text{N}_2$  (10/90) at 1 atm using an electrical furnace placed in a Labmaster 130 glovebox (Mbraun). These glass samples were inserted into the preheated furnace (at  $T_g$ ) and then treated for a given reduction duration. Afterward, they were quenched by removing them from the furnace.

**2.2. UV–vis–NIR Spectroscopy.** Usually, vanadium in glasses occurs in the states of  $\text{V}^{3+}$ ,  $\text{V}^{4+}$ , and  $\text{V}^{5+}$ . In this work, UV–vis–NIR absorption spectroscopy was used to determine the valence state of vanadium of the 0.20 mm thick samples. UV–vis–NIR spectra were recorded over the wavelength range of 300–1100 nm using a UV–vis–NIR Specord 200 spectrophotometer (Analytik Jena AG) at a resolution of 1 nm. The spectra were recorded with air as reference.

**2.3. FT-IR Spectroscopy.** The content of structurally bonded hydroxyl groups ( $\text{SiOH}$ ) was measured in the 0.20 mm thick samples using FT-IR absorption spectroscopy. FT-IR spectra were acquired by using a Vertex 70 FT-IR spectrometer (Bruker Optics) equipped with KBr beamsplitter and DLaTGS detector. The

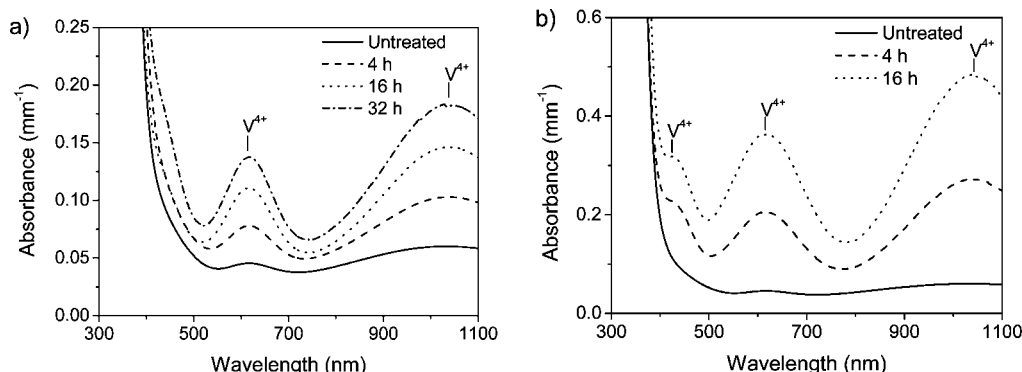


**Figure 2.** UV-vis-NIR spectra of the 0.20 mm thick glasses heated at  $T_g$  (653 °C) for various durations in (a)  $H_2/N_2$  (1/99) and (b)  $H_2/N_2$  (10/90). The bands positioned near 435, 615, and 1040 nm are all due to  $d \rightarrow d$  transitions of  $V^{4+}$ .

absorption spectra were collected in the wavenumber region from 2500 to 4000  $cm^{-1}$  using air as reference. Data had a resolution of 2  $cm^{-1}$  and were averaged over 32 scans.

**2.4. Secondary Neutral Mass Spectroscopy.** Compositional analysis of the surfaces was carried out using electron-gas secondary neutral mass spectroscopy (SNMS). The measurements were performed on an INA3 (Leybold AG) instrument equipped with a Balzers QMH511 quadrupole mass spectrometer and a Photonics SEM XP1600/14 amplifier. The analyzed area had a diameter of 5 mm and was sputtered using Kr plasma with an energy of  $\sim 500$  eV. The time dependence of the sputter profiles was converted into depth dependence by measuring the depth of the sputtered crater at 10 different directions on the same sample with a Tencor P1 profilometer.

**2.5. Microindentation.** Vickers hardness ( $H_v$ ) was measured by microindentation (Duramin 5, Struers). Twenty-five indents were made for each sample at widely separated locations with a load of 0.25 N and a hold time at the maximum load of 5 s. The lengths of the indentation diagonals were measured by using an optical microscope (reflection method).

**2.6. Differential Scanning Calorimetry.** Differential scanning calorimetry (DSC) was used to determine the  $T_g$  of the heat-treated glasses. The measurements were performed using a simultaneous thermal analyzer (Netzsch STA 449C Jupiter) on samples with a size of  $4 \times 4 \times 1$  mm<sup>3</sup>. A platinum crucible containing the sample and an empty reference platinum crucible were placed on the sample carrier of the STA at room temperature. Both crucibles were held 5 min at an initial temperature of 60 °C, and then heated at a rate of 20 °C/min to a maximum temperature of 1170 °C. Before measuring each sample, a baseline was measured by using two empty crucibles according to the above-stated heating procedure, which was used for correcting the DSC signal of the samples.

### 3. Results

**3.1. Redox State of Vanadium.** The UV-vis-NIR spectra in Figure 2 show the dependence of absorbance on heat-treatment conditions.  $V^{5+}$  has  $d^0$  electron configuration, in which only charge transfer transitions occur. These transitions are observed as strong absorption bands in the UV range,<sup>20</sup> which causes a sharp UV absorption edge. Weak bands near 615 and 1040 nm are observed in the untreated glass. These bands are assigned to  $d \rightarrow d$  transitions of  $V^{4+}$ .<sup>20,21</sup>  $V^{3+}$  has  $d \rightarrow d$  transition bands positioned at

440–460 and 650–695 nm.<sup>21,22</sup> Hence,  $V^{3+}$  cannot be detected in the spectrum of the untreated glass. On the basis of  $V^{4+}$  absorption coefficients determined by Leister et al.<sup>20</sup> for sodium silicate glasses, it is estimated that at least 80% of the vanadium is present as  $V^{5+}$  in the untreated glass. This estimation seems reasonable because the glass was melted in atmospheric air.<sup>21,23</sup>

When the glass is heat-treated in  $H_2/N_2$  (1/99), i.e., under a  $H_2$  partial pressure of 0.01 bar, the intensity of the  $V^{4+}$  bands increases with increasing  $t_a$  (Figure 2a), indicating that  $V^{5+}$  is gradually reduced to  $V^{4+}$ . In contrast, heat-treatment of the glasses in  $H_2/N_2$  (10/90), i.e., under a  $H_2$  partial pressure of 0.1 bar, results in a stronger increase in the intensity of the  $V^{4+}$  bands (Figure 2b). In addition, a band according to another  $d \rightarrow d$  transition of  $V^{4+}$  is observed at 435 nm.<sup>20,21</sup> As expected, the vanadium redox ratio shifts to the more reduced state with increasing hydrogen partial pressure in the treatment atmosphere.  $V^{3+}$  is not detected in the heat-treated glasses, but it must be noted that small amounts of  $V^{3+}$  are difficult to detect by UV-vis-NIR spectroscopy when high amounts of  $V^{4+}$  are present. The two  $V^{3+}$  bands mentioned above partly overlap with the  $V^{4+}$  bands in this region.<sup>20</sup>

**3.2. Content of Water.** The OH contents of the glasses are measured using infrared absorption bands at 3550 and 2850  $cm^{-1}$ . These bands are caused by O–H stretching vibrations of weakly and strongly hydrogen-bonded OH species, respectively.<sup>24</sup> The band at 3550  $cm^{-1}$  is asymmetric with the long tail toward lower wavenumbers.<sup>25</sup> The FT-IR spectra (Figure 3) reveal that the absorption bands of both weakly and strongly hydrogen-bonded hydroxyl species are present in all the measured glasses. However, the OH content of the glasses heat-treated in  $H_2/N_2$  is much higher than that of the original glass, i.e., the glass that was not treated. But the OH content of the glass treated in  $H_2/N_2$  (1/99) is lower than that of the glass treated in  $H_2/N_2$  (10/90) for the same temperature (653 °C) and the same duration ( $t_a$ ) of heat-treatment. This means that an increase in the hydrogen partial pressure of the treatment atmosphere leads to an increase in the permeation rate of  $H_2$ .

(22) Leister, M.; Ehrt, D. *Glass Sci. Technol.* **1999**, 72, 153.

(23) Kumar, S. *Phys. Chem. Glasses* **1964**, 5, 107.

(24) Scholze, H. *Glastech. Ber.* **1959**, 32, 81.

(25) Nakamoto, K.; Margoshes, M.; Rundle, R. E. *J. Am. Ceram. Soc.* **1955**, 77, 6480.

(20) Leister, M.; Ehrt, D.; von der Gönna, G.; Rüssel, C.; Breitbarth, F. W. *Phys. Chem. Glasses* **1999**, 40, 319.

(21) Johnston, W. D. *J. Am. Ceram. Soc.* **1965**, 48, 608.



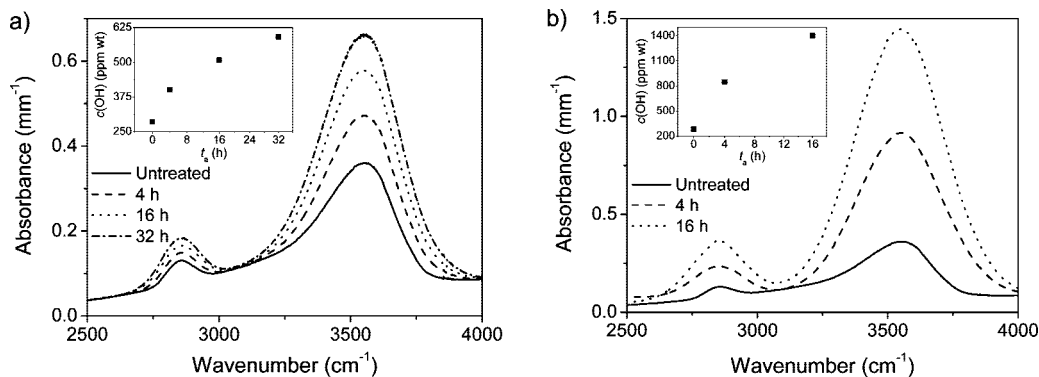


**Figure 3.** FT-IR absorption spectra of the 0.20 mm thick glasses heated at  $T_g$  (653 °C) for various durations in (a)  $H_2/N_2$  (1/99) and (b)  $H_2/N_2$  (10/90). The bands at 2850 and 3550 cm<sup>-1</sup> are caused by O–H stretching vibrations of strongly and weakly H-bonding water species, respectively. Insets: The corresponding OH contents calculated using eq (1) as a function of the heat-treatment duration ( $t_a$ ).

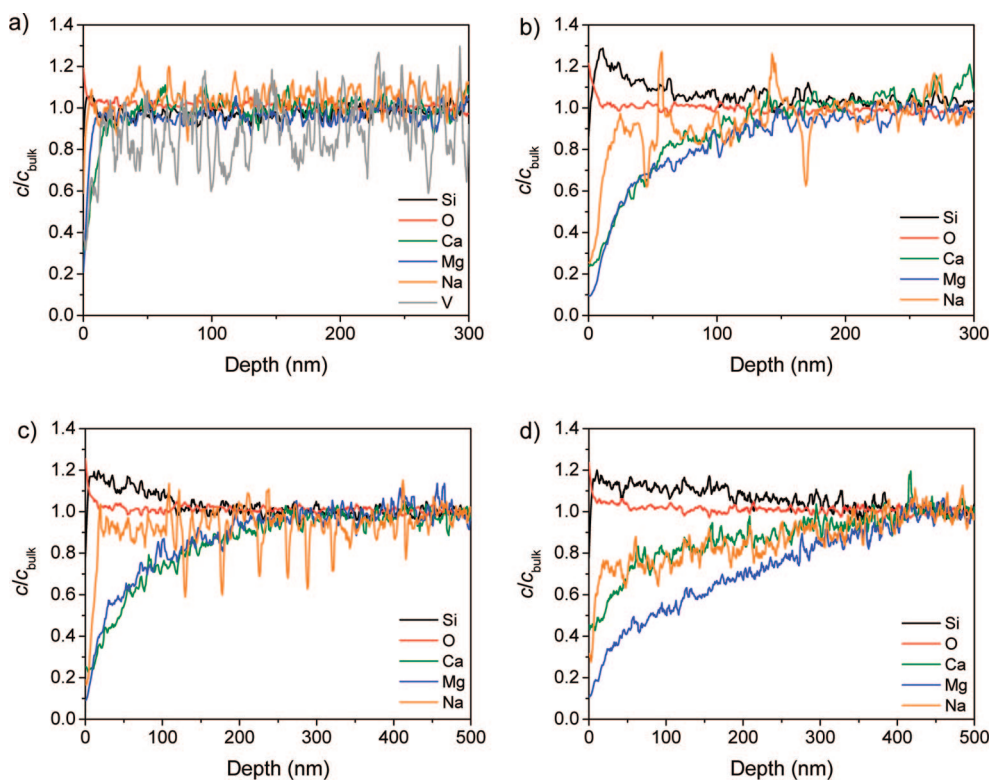


**Figure 4.** SNMS depth profiles of the (a) untreated and (b–d) heat-treated glasses. The heat treatments have been conducted in  $H_2/N_2$  (1/99) at  $T_g$  (653 °C) for (b) 4, (c) 16, and (d) 32 h. The curves are plotted as concentration of the element at a given depth divided by the concentration of the same element in the bulk of the glass ( $c/c_{\text{bulk}}$ ).

According to the model of Scholze,<sup>24</sup> the OH contents ( $c_{\text{OH}}$ ) can be estimated from the background corrected peak heights at 2850 and 3550 cm<sup>-1</sup> using the Lambert–Beer law

$$c_{\text{OH}} = \frac{M_{\text{OH}}}{\rho L_s} \left( \frac{\Delta A_{3550}}{\varepsilon_{3550}} + \frac{\Delta A_{2850}}{\varepsilon_{2850}} \right) \quad (1)$$

where  $M_{\text{OH}}$  is the molar mass of OH,  $\rho$  is the density of the glass,  $L_s$  is the sample thickness,  $\Delta A_i$  is the background-corrected absorbance, and  $\varepsilon_i$  is the molar absorption coefficient, with the subscript  $i$  denoting the band considered. Molar absorption coefficients of 112.5 and 70 L mol<sup>-1</sup> cm<sup>-1</sup> at 2850 and 3550 cm<sup>-1</sup>, respectively, for a sodium silicate glass are used for calculation of the OH content because no calibration file is available for the

studied composition.<sup>24</sup> The OH content of the untreated glass is estimated to be approximately 290 ppm and the OH contents of the heat-treated glasses are shown in the insets of Figure 3. The OH content gradually increases with increasing  $t_a$ .

**3.3. Chemical Composition Profile of the Surface Layer.** The SNMS depth profile of an untreated glass (Figure 4a) demonstrates that the concentration of the different ions is constant over the entire range of measured depths. In contrast, when the glass is heat-treated in  $H_2/N_2$  (1/99) at  $T_g$  for 4 h, it exhibits a pronounced decrease of the concentration of  $Mg^{2+}$  and  $Ca^{2+}$  toward the surface, and consequently, a clear increase of the concentration of  $Si^{4+}$  and  $O^{2-}$  toward the surface (Figure 4b). This indicates that an inward migration of  $Mg^{2+}$  and  $Ca^{2+}$

**Table 1. Vickers Hardness ( $H_v$ ) and Glass Transition Temperature ( $T_g$ ) of the Untreated Glass and the Glasses Heated at 653 °C for 16 h in  $H_2/N_2$  (1/99) and  $H_2/N_2$  (10/90)**

heat-treatment condition	$H_v$ (GPa)	$T_g$ (°C)
untreated	$8.8 \pm 0.3$	653
$H_2/N_2$ (1/99)	$9.4 \pm 0.2$	649
$H_2/N_2$ (10/90)	$8.5 \pm 0.2$	645

occurs. As a result of the inward diffusion, a silica-rich surface layer is created, the thickness of which increases with increasing  $t_a$  as seen from the depth profiles resulting from treatments at  $T_g$  for 16 h (Figure 4c) and 32 h (Figure 4d). The layer thickness is in a range from 150 to 400 nm. However, no inward migration of the earth alkaline cations occurs when the glass is heated in a hydrogen richer gas, e.g., in  $H_2/N_2$  (10/90).<sup>3</sup> Inward diffusion of  $Na^+$  is observed in two of the heat-treated samples (panels b and d in Figure 4), which contributes to the formation of the silica-rich layer. In general, the extent of the  $Mg^{2+}$  diffusion is higher than that of the  $Ca^{2+}$  and  $Na^+$  diffusion when taking the error range of data into account. The uncertainty in the detection of vanadium is relatively high because of its low concentration, and therefore, it has not been possible to evaluate whether vanadium has diffused as a result of the heat and reduction treatments.

**3.4. Impact of the Surface Modification on Hardness and Glass Transition Temperature.** Table 1 shows the effect of the thermal treatments on the Vickers hardness ( $H_v$ ) and the glass transition temperature ( $T_g$ ) of the glasses. It is seen that  $H_v$  of the glass increases after a heat-treatment in  $H_2/N_2$  (1/99), whereas  $T_g$  decreases. The glass heated in  $H_2/N_2$  (10/90) has an even lower value of  $T_g$ , whereas its hardness is not significantly different from that of the untreated glass. The reason for this will be discussed in the next section.

#### 4. Discussion

The studied glass contains Al, K, Fe, and Ti as the main impurities.  $Al_2O_3$  accounts for 0.3 wt %, but  $Al^{3+}$  ions participate in forming the glass network, so that they do not diffuse.<sup>13</sup> The concentrations of the other impurity ions are so low that they do not influence either the ionic diffusion or the reduction of vanadium.<sup>12</sup> In addition, the polishing procedure does not cause the formation of the silica-rich surface layer for the two reasons. First, the glass was ground using ethanol and polished using a diamond paste, and therefore no leaching of cations should occur. Second, the SNMS profile of untreated glass (Figure 4a) did not show any inward diffusion of cations. Therefore, the observed modification of the surface must be due to the inward diffusion of  $Mg^{2+}$ ,  $Ca^{2+}$ , and  $Na^+$  ions and/or the permeation of  $H_2$  into the glass.

As shown above, a reduction of  $V^{5+}$  to  $V^{4+}$  occurs while the glass is heat-treated in  $H_2/N_2$  (1/99). As a result, the mobile  $H_2$  species are immobilized due to formation of the structurally bonded OH groups subsequent to reaction with  $V^{5+}$ . This means that the permeation (dissolution and diffusion) of  $H_2$  is partly responsible for the  $V^{5+}$  reduction. In addition, an inward diffusion of earth alkaline cations is observed, which is coupled with the outward diffusion of

the electron holes ( $h^*$ ) as illustrated in Figure 1b. Hence, two reduction processes occur simultaneously when the glass is heat-treated in  $H_2/N_2$  (1/99): a fast process due to  $H_2$  permeation and a slower one due to outward flux of electron holes.

When the hydrogen pressure of the treatment atmosphere is raised, the  $V^{4+}$  and OH contents will increase (see Figures 2 and 3). This is attributed to the increased solubility of  $H_2$  ( $S_{H_2}$ ) in the glass at higher pressures. For example,  $S_{H_2}$  is proportional to the hydrogen pressure raised to the power of 1.28 for a natural rhyolitic obsidian.<sup>2</sup> The lack of inward diffusion of earth alkaline cations in the glasses heated in  $H_2/N_2$  (10/90) indicates that the hydrogen pressure is so high that all  $V^{5+}$  ions are reduced entirely by  $H_2$  molecules before the earth alkaline cations start to diffuse. In fact, the inward diffusion process, caused by the outward diffusion of  $h^*$  when  $V^{5+}$  is reduced, is  $\sim 280$  times slower compared to the  $H_2$  permeation process at the high  $H_2$  pressure of 0.10 bar.<sup>3</sup> Using the tarnishing model<sup>4,8–10</sup> and the permeation rate of  $H_2$  in an iron-containing glass of very similar composition,<sup>3</sup> the thickness of the  $H_2$  permeated layer is calculated to be  $\sim 40 \mu m$  for the glass heat-treated in  $H_2/N_2$  (10/90) at  $T_g$  for 32 h. On the other hand, when the glass is heated in  $H_2/N_2$  (1/99), there are insufficient  $H_2$  species available to reduce all of the  $V^{5+}$  ions and this leads to the observed inward diffusion of  $Mg^{2+}$  and  $Ca^{2+}$ .

Inward diffusion of  $Na^+$  is also observed, but the diffusion depth of  $Na^+$  is smaller than that of the earth alkaline ions. This is an interesting phenomenon because alkali ions are normally found to be faster than earth alkaline ions in glasses because of their lower charge. The inward diffusion occurs to charge-balance the outward flux of electron holes, and the charge might be most effectively transferred by the divalent cations.

By comparison of the  $T_g$  values in Table 1 with the OH contents in Figure 3, it is realized that  $T_g$  decreases with increasing OH content. In other words, the permeation of  $H_2$  has caused the decrease in  $T_g$ . This phenomenon is well-known.<sup>26</sup> For example,  $T_g$  of soda-lime-silica glasses decreases by  $\sim 4$  K for every 0.01 wt % of water in the glass.<sup>27</sup> The effect has been attributed to conversion of bridging oxygens to nonbridging hydroxyls.

As shown in Table 1, the glass heated in  $H_2/N_2$  (1/99) is harder than the untreated glass due to the formation of a silica-rich nanolayer on its surface. The ratio of the indentation diagonal length to the depth for a Vickers diamond is 7:1. As the length of the indentation diagonal was  $7.1 \mu m$  for the untreated glass, the indentation depth is  $1.0 \mu m$ . Hence, the indenter penetrates the modified layer and reaches into the original glass. This is why the hardness is not as high as that of a pure  $SiO_2$  glass (OH content: 150 ppm) that was measured to having a hardness of  $11.3 \pm 0.3$  GPa at 0.25 N. In addition, the modified layer is not solely composed of silica. Finally, the increased network connectivity caused by the inward diffusion of the network modifying cations may to some extent be counteracted by the perme-

(26) Deubener, J.; Müller, R.; Behrens, H.; Heide, G. *J. Non-Cryst. Solids* **2003**, 330, 268.

(27) Rapp, D. B.; Shelby, J. E. *Phys. Chem. Glasses* **2003**, 44, 393.

ation of  $H_2$  into the glass as this permeation results in the breaking of Si–O bonds. The dependence of hardness on the heat-treatment under the reducing condition is in good agreement with that reported elsewhere.<sup>3</sup> For instance, heat-treatment of an iron-bearing glass in  $H_2/N_2$  (1/99) results in inward diffusion of divalent cations, and hence formation of a silica-rich surface. The chemical durability of the iron-bearing glass increases as a result of the treatment.

The question arises whether this type of reduction-induced diffusion can occur in other glass systems and glass-ceramics containing vanadium in an oxidized state. A prerequisite is the presence of mono- or divalent cations as these ions represent the mobile ions in glasses. The mobility of earth alkaline ions increases with increasing alkali content.<sup>28</sup> This should result in a thicker silica-rich surface layer with increasing alkali content for a given heat-treatment condition, but increasing the alkali content at the same time decreases the hardness and chemical durability, i.e., it is necessary to find the optimum alkali content. For the reduction of iron, the layer thickness increases with increasing iron content as more electron holes move when more  $Fe^{3+}$  ions are reduced to  $Fe^{2+}$ .<sup>3</sup> A similar effect is expected for vanadium. It would be interesting to study whether the reduction-induced diffusion can occur in vanadium-bearing glass-ceramics. For example, it would be of interest if it occurs in  $Li_2O-Al_2O_3-SiO_2$  glass-ceramics as these materials contain  $\sim 1$  wt %  $V_2O_5$  and have a low thermal expansion coefficient.<sup>29</sup>

## 5. Conclusions

Reduction of vanadium in a silicate glass by hydrogen operates by permeation of  $H_2$  into the glass when heated in  $H_2/N_2$  (10/90) which leads to a reduction zone thicker than  $10\ \mu m$  and by both  $H_2$  permeation and outward flux of electron holes when heated in  $H_2/N_2$  (1/99). The motion of the electron holes is charge-compensated by an inward diffusion of the mobile network-modifying cations (primarily  $Mg^{2+}$  and  $Ca^{2+}$ ). This diffusion leads to formation of a silica-rich nanolayer on the surface. Hence, a glass surface enriched in silica can be created by the following steps: (1) Adding vanadium oxide into a silicate glass batch. (2) Melting the batch in atmospheric air to increase the  $V^{5+}$  content of the glass. (3) Heat-treating the glass under  $H_2/N_2$  (1/99) at  $T_g$  to reduce  $V^{5+}$  to  $V^{4+}$ , and hence induce the inward diffusion, and finally form the silica-rich surface layer. The formation of structurally bonded OH groups results in lower  $T_g$ , whereas the surface layer makes the glass harder. The approach presented here is a supplemental tool to surface coating for creating functional surfaces on glassy materials.

**Acknowledgment.** The authors thank Thomas Peter (Clausthal University of Technology) for performing SNMS measurements and Martin Jensen (Aalborg University) for critical reading of the manuscript.

CM802513R

(28) Natrup, F. V.; Bracht, H.; Murugavel, S.; Roling, B. *Phys. Chem. Chem. Phys.* **2005**, *7*, 2279.

(29) Comte, M. J. M.; Netter, P. L.; Ricoult, D. L. G. U.S. Patent 5 070 045, 1991.